Combined Supplementary Materials

Figure-S1, related to Figure 1

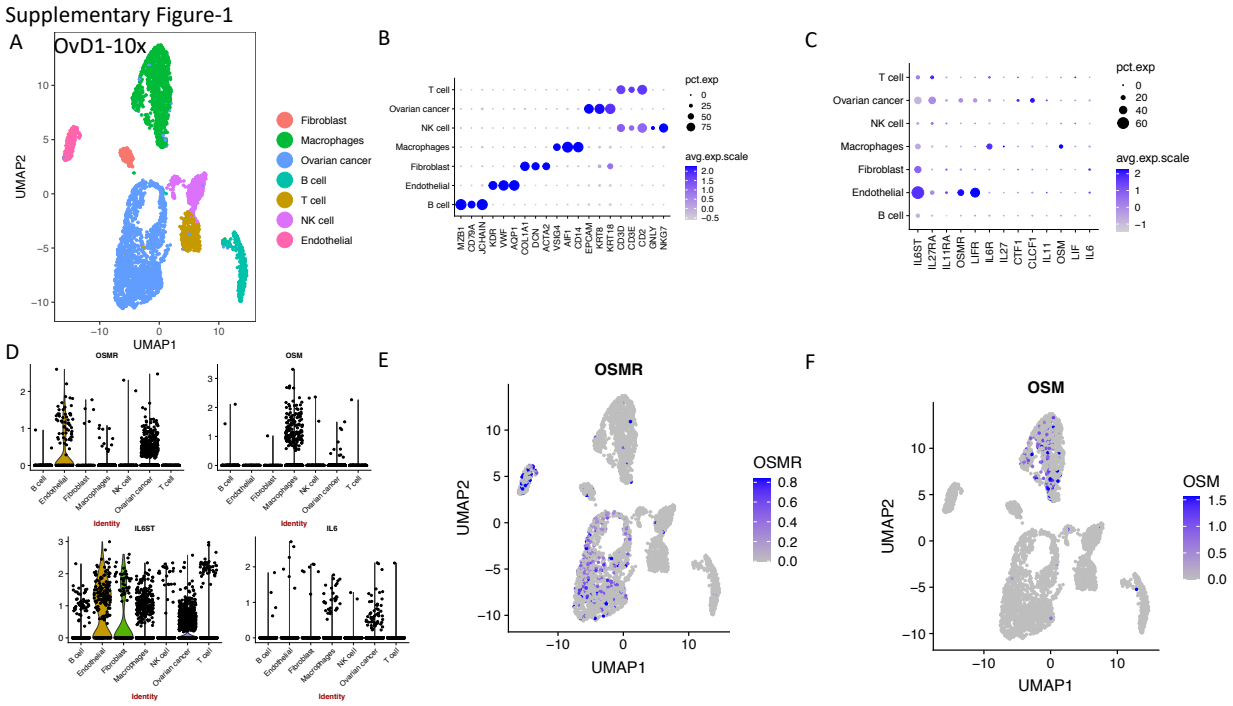

Figure-S1. OvD1-10x scRNA-seq dataset. A, UMAP plot of different cell types detected in the dataset. **B,** Dotplot of cell type marker expression in different cell types showing their average expression (color of dot) and percentage of cells with gene expression (size of dot). **C,** Dotplot of IL6 family receptors and ligands expression present in the dataset. **D**, Violin plots of selected receptors and ligands expression in each cell type. **E,** UMAP plot showing expression of OSMR in each cell in the dataset. **F**, UMAP plot showing expression of OSM in each cell in the dataset.

Figure-S2, related to Figure 1

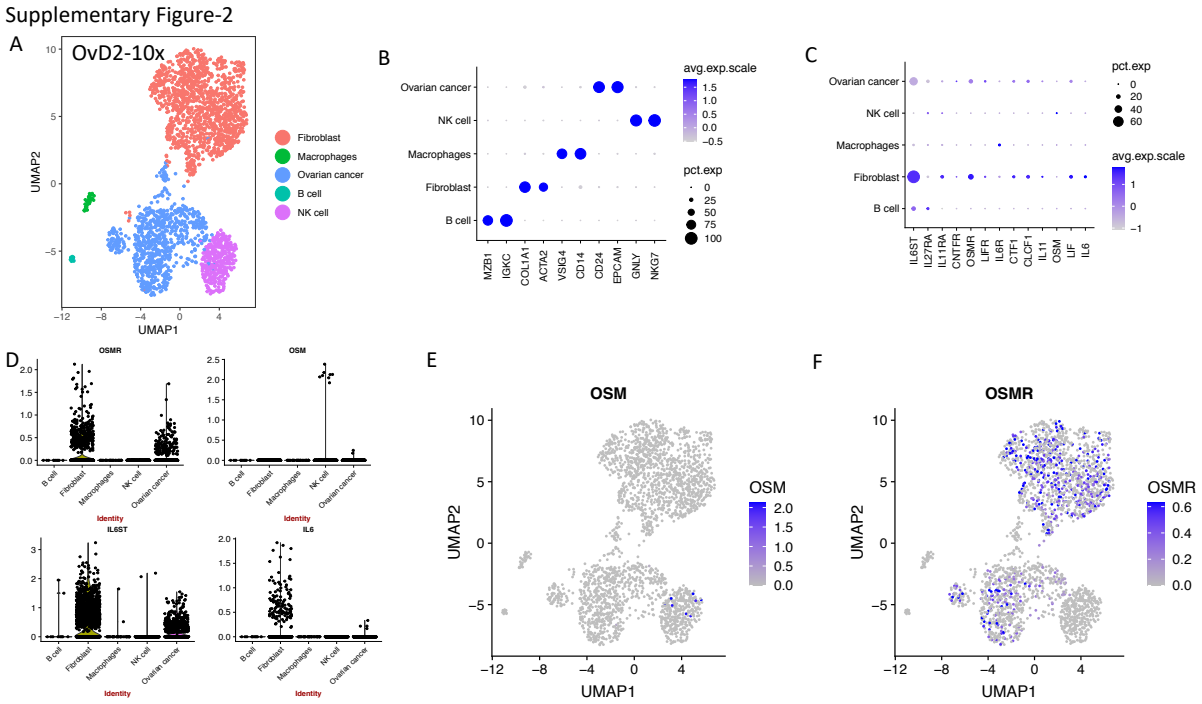

Figure-S2. OvD2-10x scRNA-seq dataset. A, UMAP plot of different cell types detected in the dataset. **B,** Dotplot of cell type marker expression in different cell types showing their strength (color of dot) and prevalence (size of dot). **C,** Dotplot of IL6 family receptors and ligands expression present in the dataset. **D,** Violin plots of selected receptors and ligands expression in each cell type. **E,** UMAP plot showing expression of OSMR in each cell in the dataset. **F,** UMAP plot showing expression of OSM in each cell in the dataset.

Figure-S3, related to Figure 1

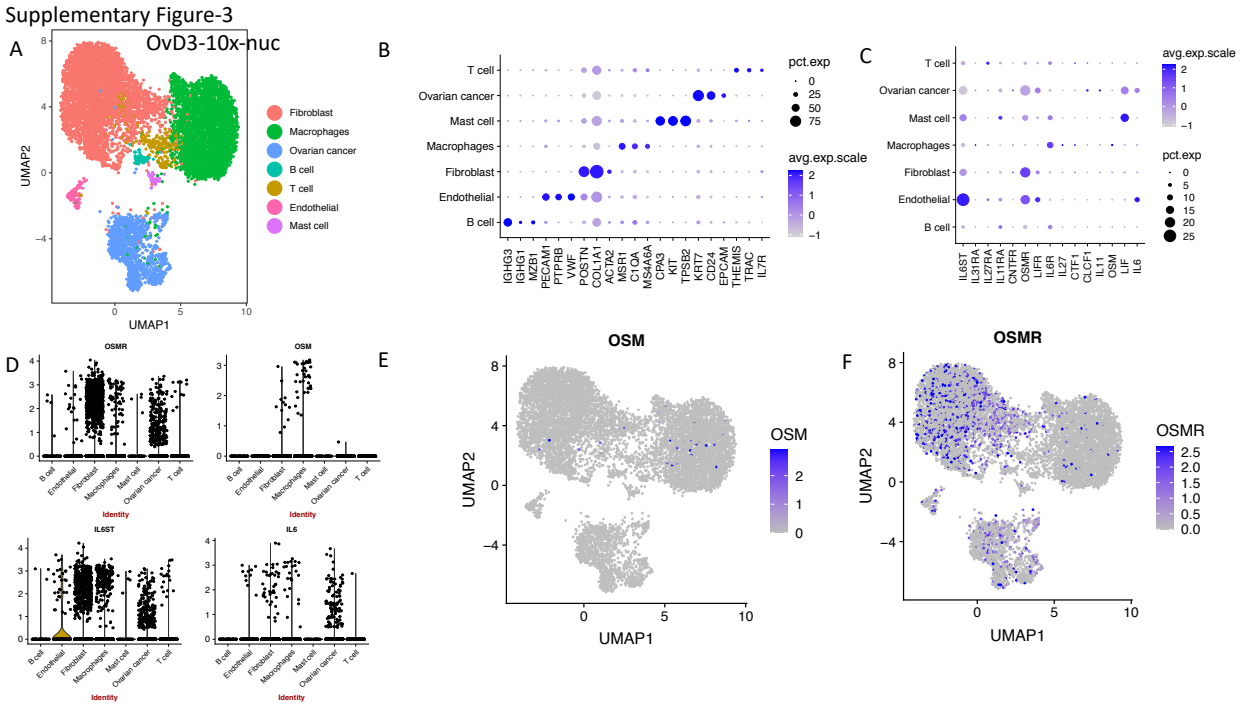

Figure-S3. OvD3-10x-nuc snRNA-seq dataset. A, UMAP plot of different cell types detected in the dataset. **B,** Dotplot of cell type marker expression in the different cell types showing their strength (color of dot) and prevalence (size of dot). **C,** Dotplot of IL6 family receptors and ligands expression present in the dataset. **D,** Violin plots of selected receptors and ligands expression in each cell type. **E,** UMAP plot showing expression of OSMR in each cell in the dataset. **F,** UMAP plot showing expression of OSM in each cell in the dataset.

Figure-S4, related to Figure 1

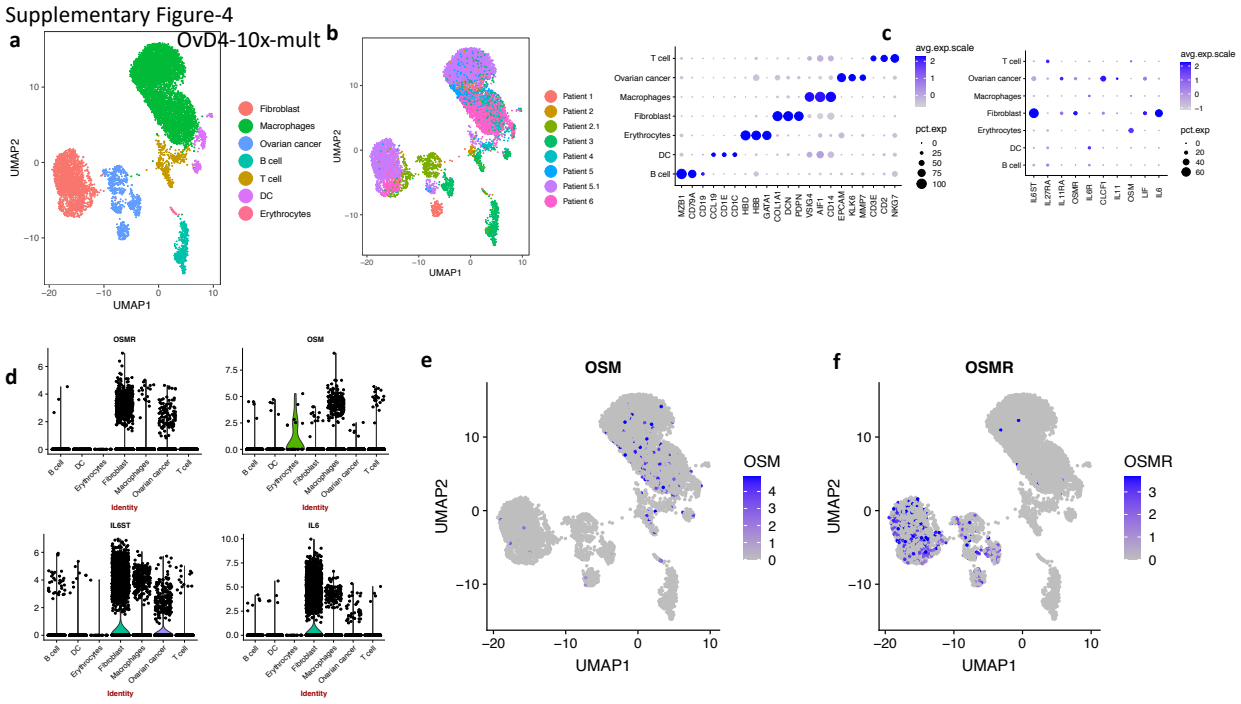

Figure-S4. OvD4-10x-mult multiple-patient scRNA-seq dataset. A, UMAP plot of different cell types detected in dataset. **B,** Dotplot of cell type marker expression in the different cell types showing their strength (color of dot) and prevalence (size of dot). **C,** Dotplot of IL6 family receptors and ligands expression present in the dataset. **D,** Violin plots of selected receptors and ligands expression in each cell type. **E,** UMAP plot showing expression of OSMR in each cell in the dataset. **F,** UMAP plot showing expression of OSM in each cell in the dataset.

Figure-S5, related to Figure 1

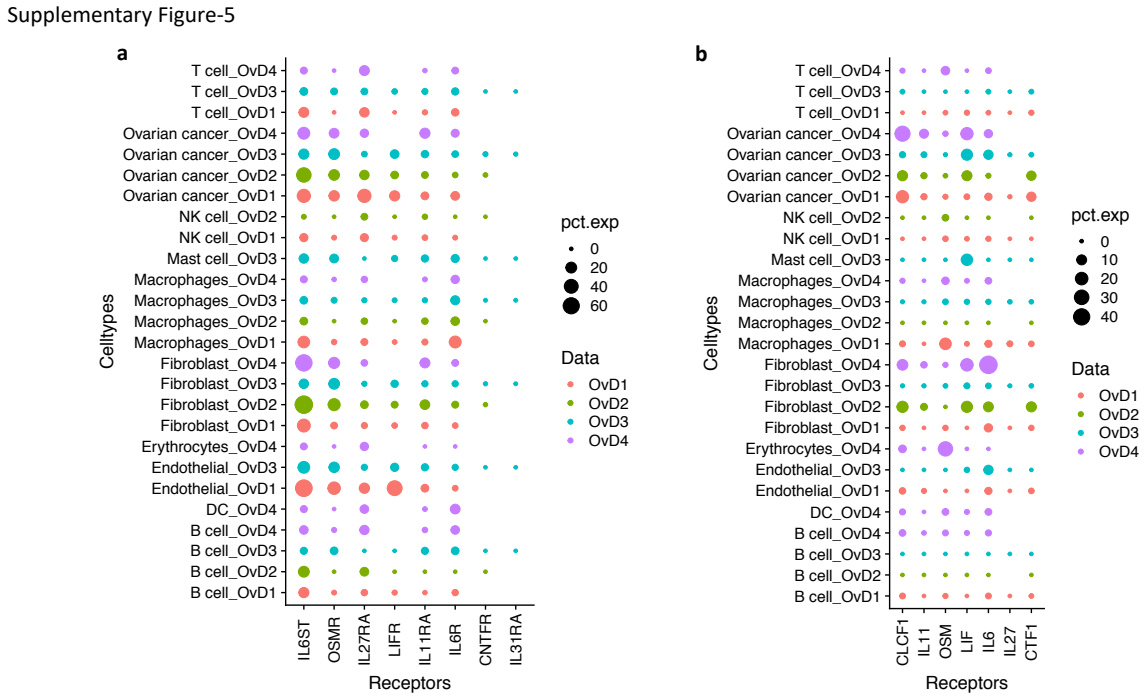

Figure-S5; Related to Figure-1. A, Dotplot showing the average expression of IL6 family receptors in each cell type in from each of the four datasets. Size of the dots show the percentage of cells in each cell type showing expression. Color of the dots show the datasets. **B,** Dotplot showing the expression of IL6 family ligands in each cell type in each of the four datasets. Size of the dots show the percentage of cells in each cell type showing expression. Color of the dots represent the datasets.

Figure-S6, related to Figure 1

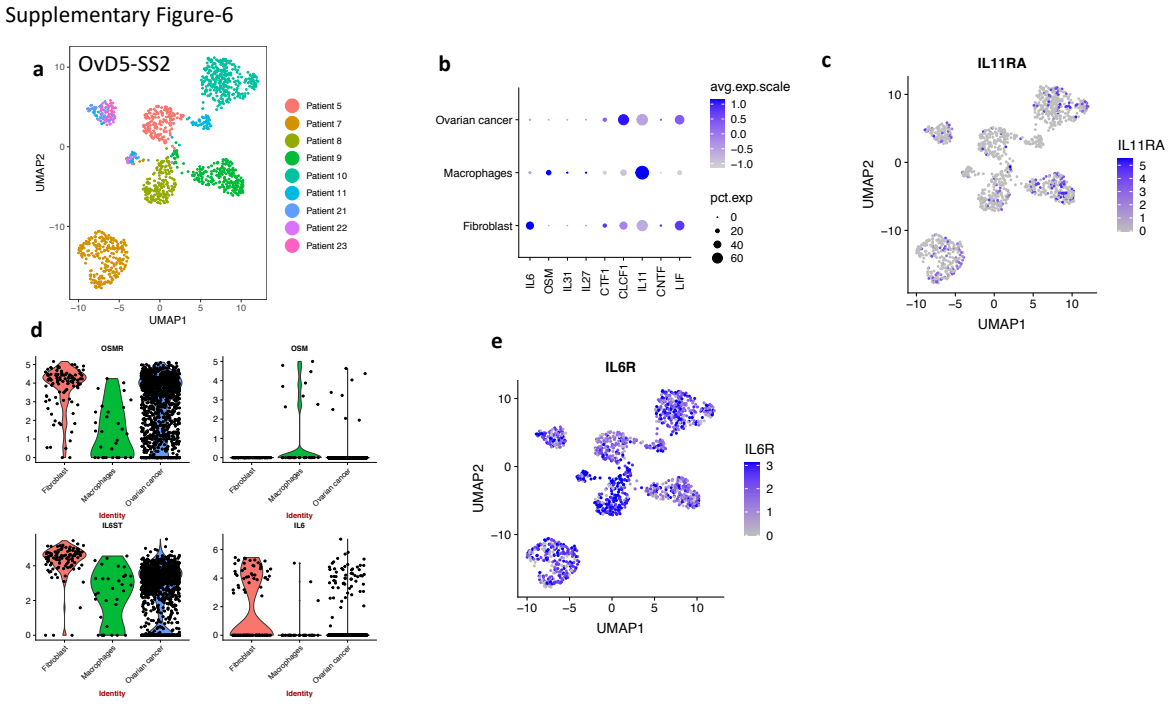

Figure-S6. OvD5-SS2 multiple-patient SS2 dataset. A, UMAP plot of the cells colored based on different patients in the dataset. **B,** Dotplot of IL6 family receptors and ligands expression present in the dataset showing their strength (color of dot) and prevalence (size of dot). **C,** UMAP plot showing expression of IL11RA in each cell in the dataset. **D,** Violin plots of selected receptors and ligands expression in each cell type. **E,** UMAP plot showing expression of IL6R in each cell in the dataset.

Figure-S7, related to Figure 1 and 2.

Supplementary Fig 7

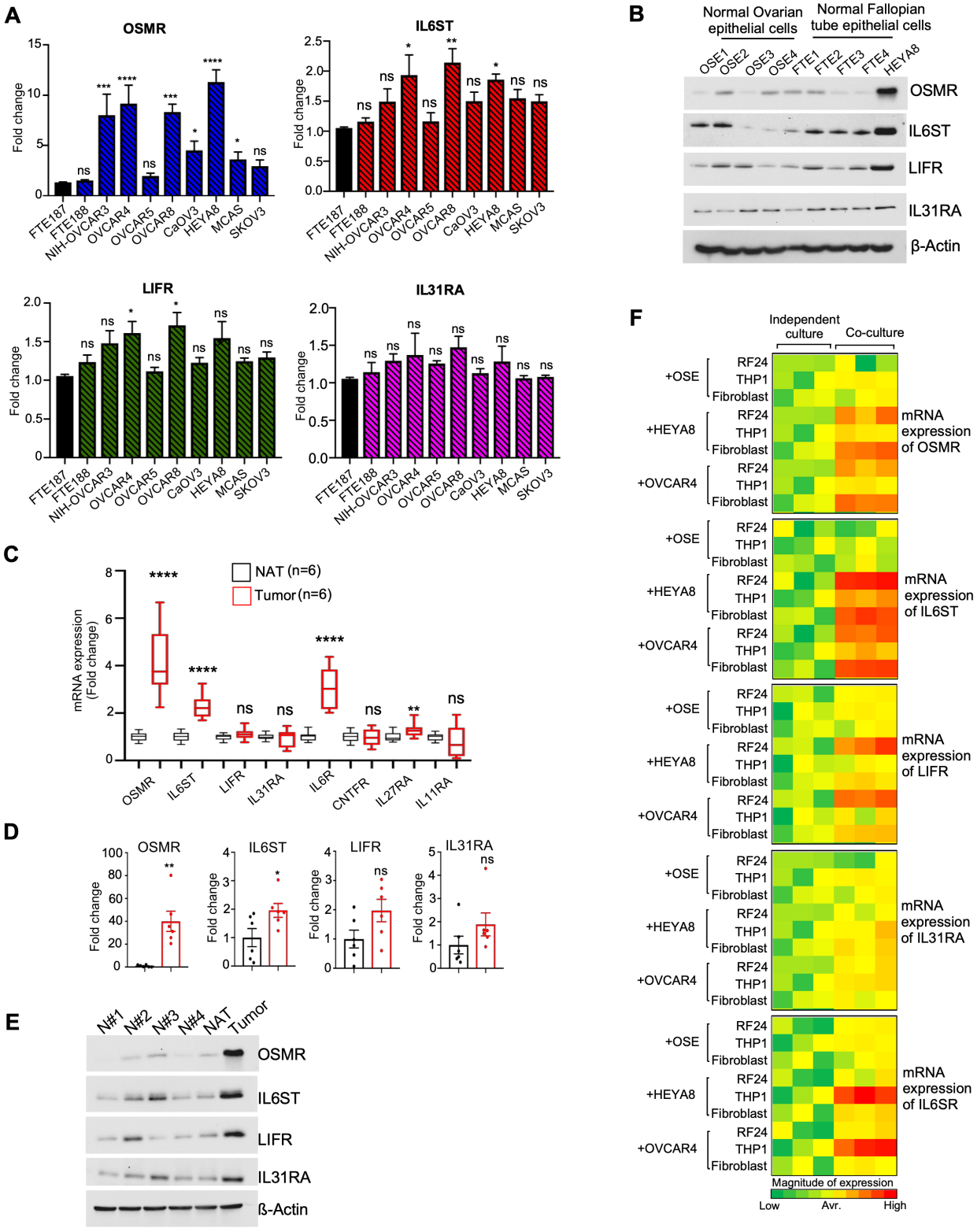

Figure S7. OSMR is highly expressed in ovarian cancer cells and cancer tissues compared to normal cells and tissues. A, Total protein was isolated from different ovarian cancer cell lines and fallopian tube epithelial cells (FTE) and western blotting was performed. Histograms represent protein levels of the indicated proteins normalized to β-Actin and w.r.t FTE 187 cells from three independent experiments of Fig 2A. **B,** Total protein was isolated from 4 normal surface epithelial cells (OSE) and 4 fallopian tube epithelial cells (FTE) and western blotting was performed with the indicated antibodies. HEYA8 having high OSMR expression is used for comparison. **C,** qPCR showing mRNA expression of the indicated IL6 family receptors in ovarian tumor tissues and their matched normal adjacent ovarian tissues (NAT) from 6 patients (n=6). **D,** Total protein was isolated from 6 different normal adjacent ovarian tissues (NAT) and 6 tumor tissues and western blotting was performed. Histograms represent protein levels of the indicated proteins from 6 tissues in each group normalized to β-Actin and with respect to NAT as in Fig 2B. **E,** Cell lysates were prepared from normal ovarian tissues (N) (n=4), a representative of normal adjacent tissue (NAT) and tumor tissue were included for comparison and western blotting was performed with indicated antibodies. **F,** Heatmap shows mRNA expression of the indicated IL6 family receptors in fibroblasts (GM15859), macrophages (THP1) and endothelial cell (RF24) which were seeded in the bottom chamber of trans-well inserts, when cultured alone or co-cultured with ovarian surface epithelial cells (OSE), HEYA8 or OVCAR4. OSE, HEYA8 and OVCAR4 cells were seeded on the upper chamber of trans-wells of size 1 μm. Total RNA was isolated from both the cultures and mRNA expression of indicated genes were determined with respect to β-Actin. Color codes at the bottom indicate the magnitude of gene expression. Data

represent means ± SEM. Student's t test (two tailed, unpaired) was performed **in** A, C, and D respectively**.** ****P≤ 0.0001, ***P≤0.001, **P≤0.01, *P≤0.05, ns: not significant.

Figure-S8, related to Figure 1

Supplementary Fig 8

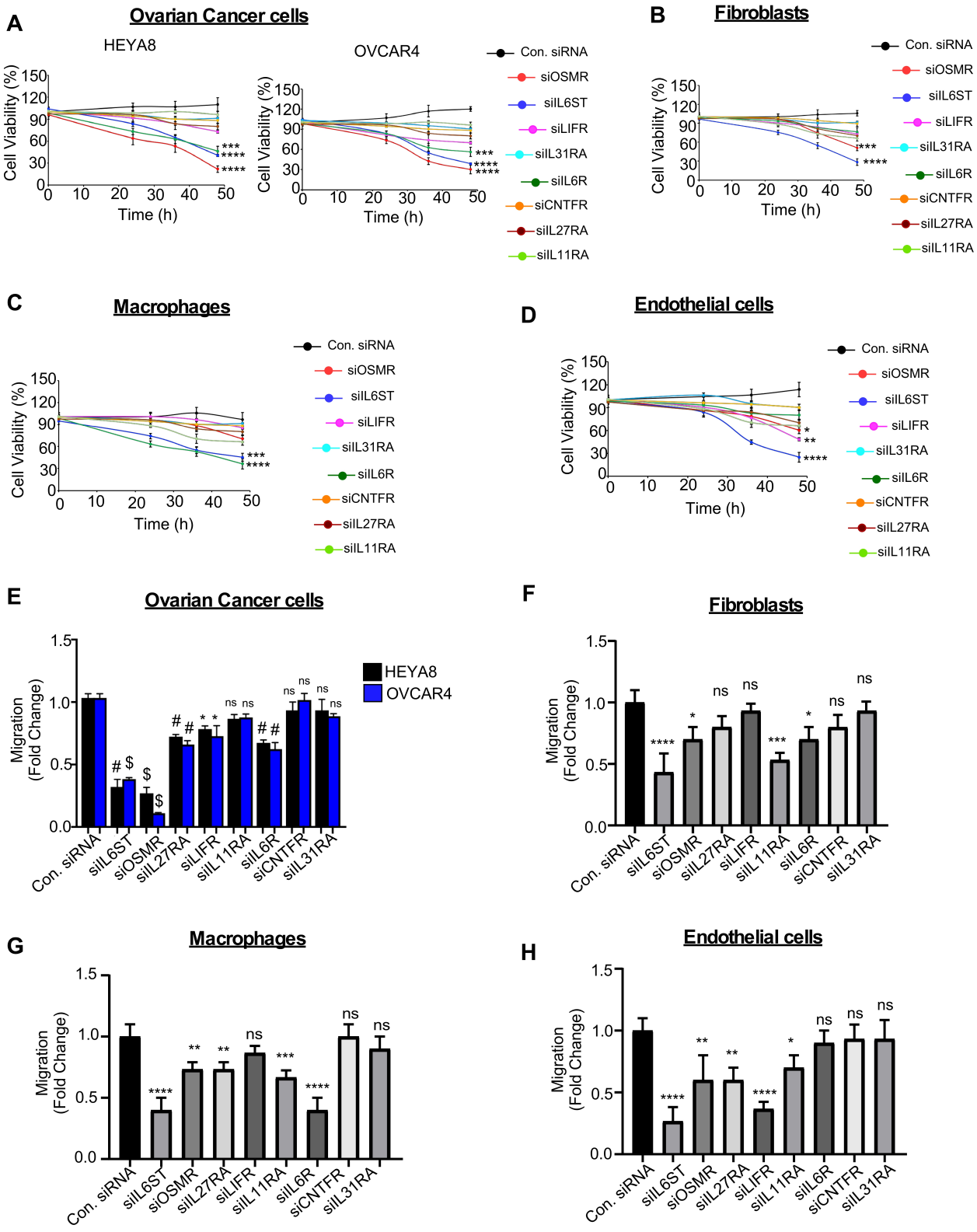

Fig. S8. Knockdown of OSMR significantly inhibit the proliferation and migration of ovarian cancer cells and fibroblasts. A-D, CCK8 assay demonstrating proliferation in ovarian cancer cells (HEYA8 and OVCAR4), fibroblasts, macrophages (THP1), and Endothelial cells (RF24). Cells were transfected with indicated siRNA of IL6 family receptors for 24h and CCK8 proliferation assay was performed at the indicated time points. **E-H** Trans-well migration assay in ovarian cancer cells (HEYA8 and OVCAR4), Macrophages (THP1), Endothelial cells (RF24) and Fibroblasts cells. Cells were transfected with indicated siRNA of IL6 family receptors for 24h and migration assay was performed for 12h. Student's t test (two tailed, unpaired) was performed in **(A-H)** w.r.t control siRNA**.** Data represent means ± SEM. ****P≤ 0.0001, ***P≤0.001, **P≤0.01, *P≤ 0.05, $^{\#}$P≤0.001, $^{\$}$P≤ 0.0001, ns: not significant.

Figure-S9, related to Figure 2

Supplementary Fig 9

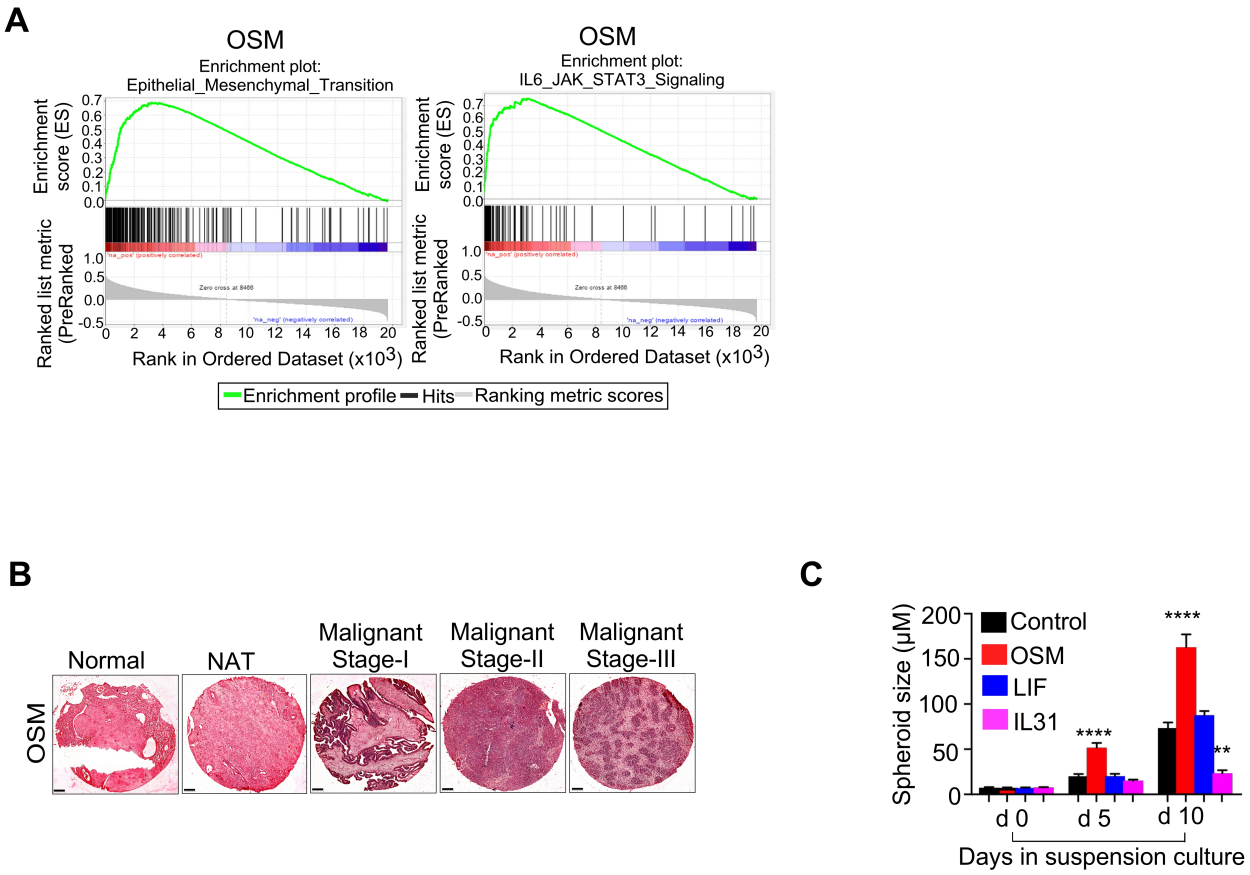

Fig. S9. OSMR expression is associated with malignant characteristics in ovarian cancer. A, GSEA analysis demonstrating the enrichment score of indicated functional annotation marks based on OSM expression in the TCGA ovarian cancer samples. ES: enrichment score, NES: normalized enrichment score. **B,** Representative images from ovarian cancer tissue microarray core showing OSM expression immunostained for OSM and scanned using Aperio Scan Scope (Aperio Technologies). Normal (N), Normal adjacent tumor (NAT), Malignant stage I, II and III are marked. Scale bar, 100 µm. **C,** Histogram shows the relative size of spheroids as in (Fig-2I) at the indicated time points.

Student's t test and Dunnett's multiple comparison test were performed in **(C)**. Data represent means ± SEM. ****P≤ 0.0001, and **P≤0.01

Figure-S10, related to Figure 2

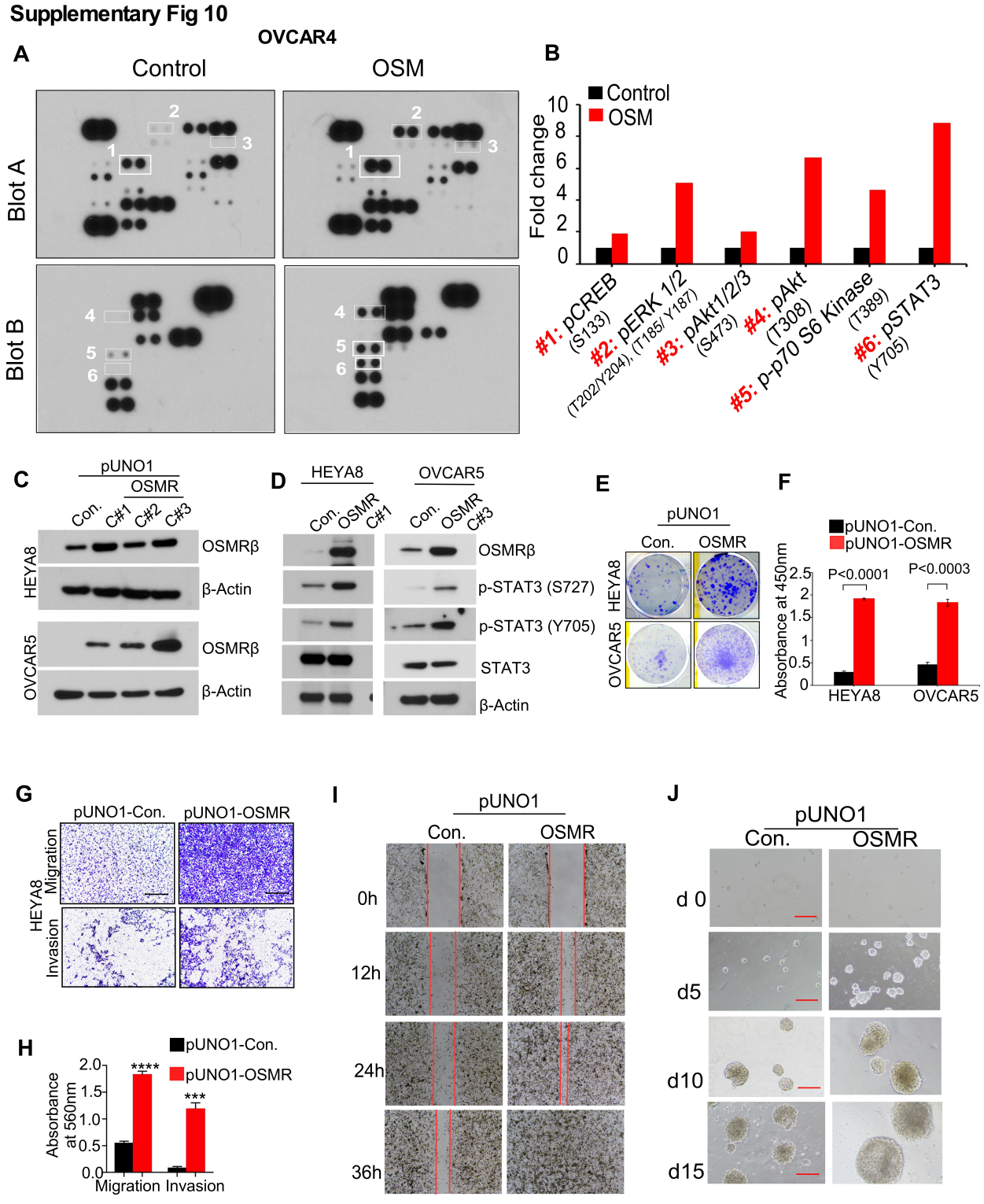

Fig. S10. High OSMR expression promotes oncogenic signaling in ovarian cancer. **A,** OVCAR4 cells were stimulated with OSM for 24h and cell lysates were prepared, and the levels of phospho-kinase proteins were quantitated using Phospho-protein kinase array membrane. **B,** the histograms represent mean values of densitometry readings of the significantly altered Phospho-kinase proteins on the array membrane marked in white squares. **C,** HEYA8 and OVCAR5 cells were stably transfected with pUNO1-OSMR overexpression plasmid. C#1 to C#3 refers to different clones selected after stable transfection and western blot was performed for the indicated proteins. **D,** HEYA8 and OVCAR5 were stably transfected with clone #1 and clone#3 respectively and western blot was performed for the indicated proteins. **E,** HEYA8 and OVCAR5 cells were stably transfected with pUNO-1-OSMR overexpression plasmid and 1200 cells were seeded on 6 well plate for colony forming assay. Colonies were stained with 0.5% crystal violet and photographed on Day 10. **F,** Crystal violet-stained colonies were eluted in 10% acetic acid and quantitated. **G,** HEYA8 cells stably overexpressed with pUNO1-Control vector and clone #1 of pUNO1-OSMR were seeded for 12 h and 16h for migration and invasion respectively. Scale bar, 100 μm. **H,** Crystal violet-stained migrated and invaded cells were eluted in 10% acetic acid and quantitated. **I,** Wound healing assay in HEYA8 stably overexpressed with pUNO1-Control vector and clone #1 of pUNO1-OSMR and photographed at indicated time points. **J,** Representative images of 3D spheroid formation assay. HEYA8 cells stably overexpressed with pUNO1-OSMR were cultured in Clona Cell media on low adherent plate and photographed at indicated days. Scale bar, 500 μm. Student's t test (two tailed, unpaired) was performed in **(F, H)**. Data represent means ± SEM. ****$P \leq 0.0001$, ***$P \leq 0.001$

Figure-S11, related to Figure 3

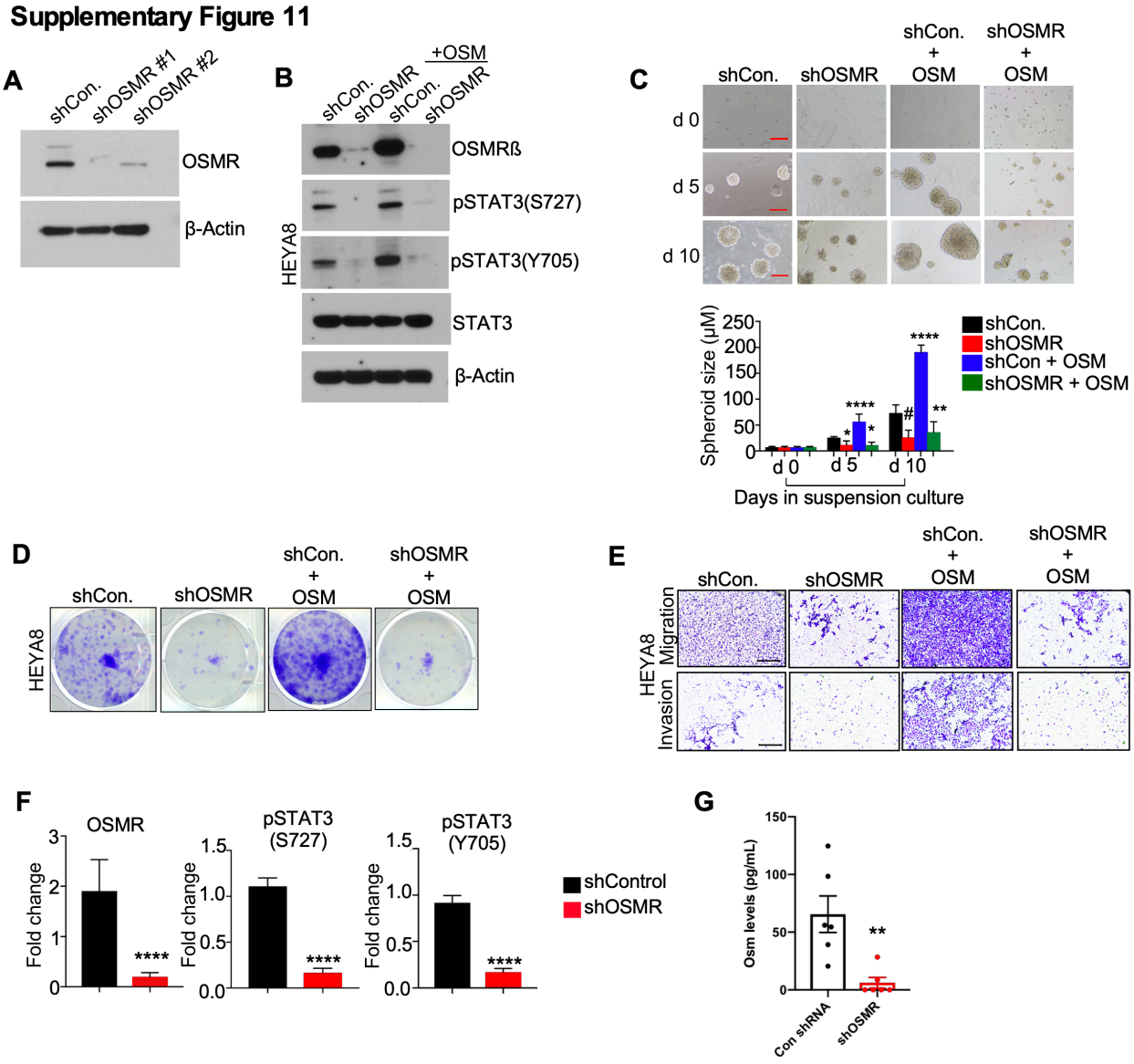

Fig. S11. Knockdown of OSMR reduced ovarian cancer progression and abrogates expression of downstream targets. A, HEYA8 cells were stably transfected with two non-overlapping shOSMR-lenti vectors, shOSMR #1 and shOSMR#2. Cells lysates were prepared after 48h and western blotting was performed for the indicated proteins. **B,** HEYA8 cells stably knocked of OSMR using shRNA or express con-shRNA were stimulated with OSM (100ng/mL) for 48h. Cell lysates were then prepared, and western

blot was performed for the indicated proteins. **C,** Representative images of 3D spheroid formation assay. HEYA8 cells stably express shControl or shOSMR#1 were cultured in ClonaCell media on low adherent plate with or without OSM (100ng/mL) for the indicated time. Spheroids were photographed at indicated days. Scale bar, 500 μm. Histogram represents size of spheroids from 4 different fields per group from Day 0 to Day 10 of spheroid culture. **D,** HEYA8 cells from C were treated with OSM for 14-days, then stained using crystal violet staining to visualize colonies. **E,** HEYA8 cells from C were stimulated with and without OSM for 12 h. Scale bar, 100 μm. **F,** Histograms represent densitometric analysis of OSMR protein levels and STAT3 phosphorylation levels in tumor tissues collected from sh-control-HEYA8 and sh-OSMR-HEYA8 injected nude mice in **Fig. 3I**. Error bars indicate three representative tissues collected for Western blot. **G,** BR-Luc murine cell lines that were stably depleted for OSMR using shOSMR or the control cells were injected intraperitoneally in syngeneic FVB mice (n= 6/group). Ascites fluid was collected after 6-weeks of injection. Peritoneal wash was performed using 3 ml of PBS in the mice exhibit either low or no ascites, then OSM levels were determined by ELISA. Data represent the means ± SEM of six mice from each group. Student's t test (two tailed, unpaired) was performed to determine P-Value. Data represent means ± SEM. ****$P \leq 0.0001$, $^{\#}P \leq 0.001$, **$P \leq 0.01$, *$P \leq 0.05$.

Figure-S12, related to Figure 3

Supplementary Fig 12

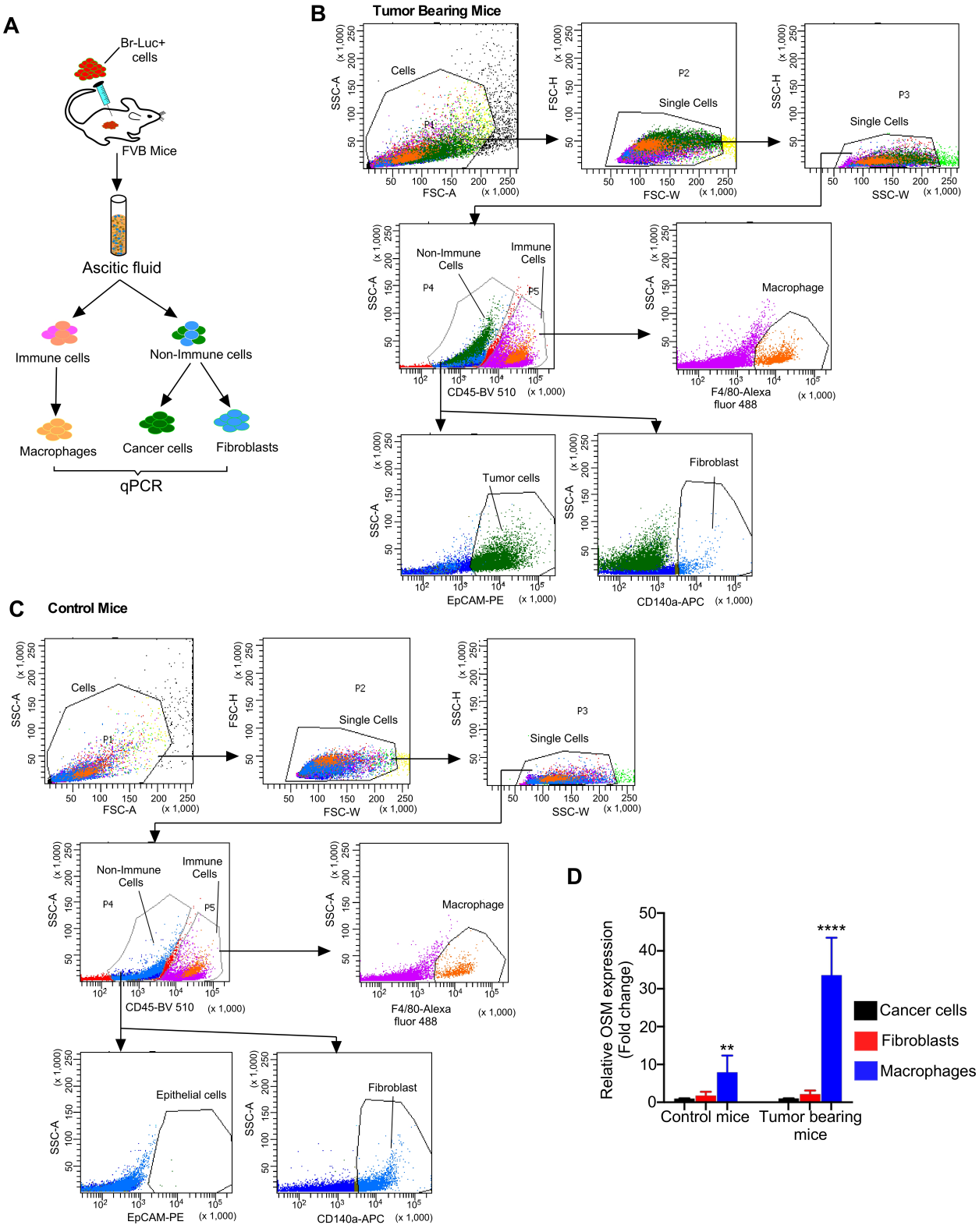

Fig. S12. Peritoneal macrophages express high levels of OSM. A, Schema shows the flow chart how macrophages, fibroblast and epithelial cells were collected from mice for qPCR. Single cell preparations were gated for respective markers as labelled. First, we sorted the CD45+ immune cells and macrophages using Alexa Fluor 488 F4/80 labelled antibody, then CD140a+ fibroblasts and EpCAM+ tumor cells were sorted. **B-C,** macrophages, fibroblasts and tumor/epithelial cells from tumor bearing mice (B) and non-tumor bearing control mice (C) were collected from ascitic fluid or peritoneal wash respectively. **D,** Total RNA was prepared from the indicated cells and qPCR was performed to determine the mRNA levels of OSM in each population. One-way ANOVA was performed**.** Data represent means ± SEM. ****$P \leq 0.0001$, **$P \leq 0.01$

Figure-S13, related to Figure 4.

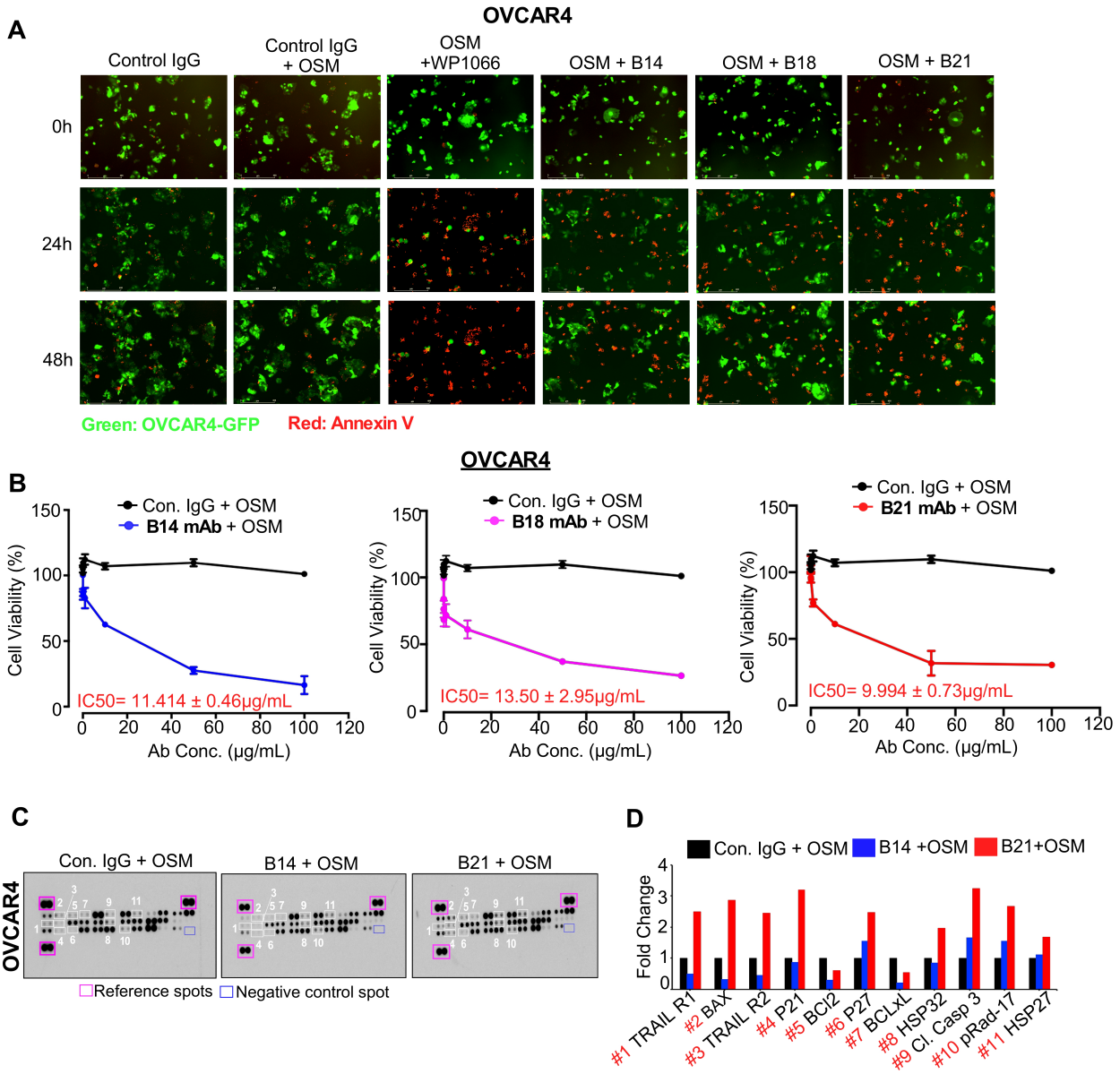

Fig. S13. OSMR monoclonal antibodies abrogate OSM mediated ovarian cancer cell proliferation and induces apoptosis. A, Representative phase contrast images of 'Fig- 4b' showing OVCAR4-GFP+ cells (green; viable cells) and Annexin V Red+ cells (Red; apoptotic cells) per field using Incucyte Live cell analyzer for a period of 0-48h. Scale bar, 400µm. **B,** OVCAR4 cells were treated with indicated concentrations of top 3

selected anti-OSMR antibodies B14, B18 and B21 with OSM stimulation and cell viability was assessed by CCK8 cell viability assay after 48h of treatment and IC50 of antibodies were calculated using GraphPad software. **C,** Human Apoptosis Protein array membrane shows the levels of proteins associated with cell death and are altered upon the treatment of B14 and B21 anti-OSMR antibodies in the presence of OSM for 48h in OVCAR-4 cells. **D,** Histogram shows the mean densitometry readings of the proteins marked by white squares on array membrane. Student's t test (two tailed, unpaired) was performed. Data represent means ± SEM.

Figure-S14, related to Figure 4.

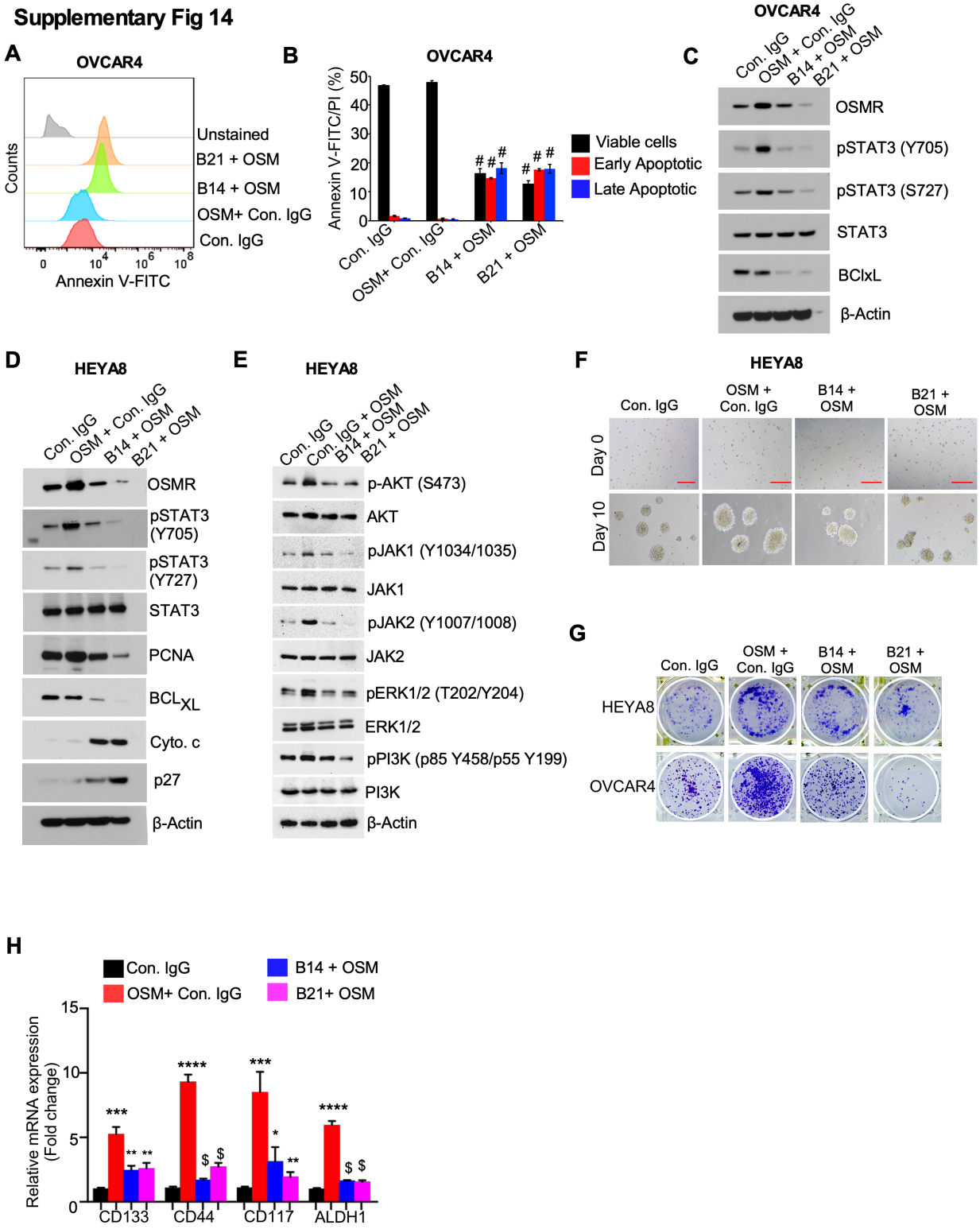

Fig. S14. Anti-OSMR antibodies inhibit oncogenic signaling in ovarian cancer cells. **A,** Annexin V-FITC/PI apoptosis detection by Flow cytometry in HEYA8 cells pre-treated with B14 or B21 monoclonal antibodies for 4h, then stimulated with OSM (100ng/mL) for 16 h. **B,** Histogram represent the viable (Annexin V-FITC negative and PI negative), early (Annexin V-FITC positive and PI negative) and late apoptotic cells (Annexin V-FITC positive and PI positive). **C-E,** OVCAR4 and HEYA8 cells were treated with B14 (10ug/mL) and B21 (10ug/mL) monoclonal antibodies for 4h followed by stimulation of OSM (100ng/mL) for 48h. Cell lysates were then collected, and western blot was performed for the indicated proteins. **F,** Representative images of 3D spheroid formation assay. HEYA8 cells were treated with B14 and B21 (10ug/mL each) anti-OSMR antibodies for 4h followed by stimulation of OSM (100ng/mL). The spheroids were photographed for indicated days. Scale bar, 500 μm. **G,** Representative images of colony formation assay in HEYA8 and OVCAR4 cells treated with B14 and B21 anti-OSMR antibodies in presence of OSM (100ng/mL) for 10 days. **H,** HEYA8 cells were treated with B14 (10ug/mL) and B21 (10ug/mL) monoclonal antibodies for 4h followed by stimulation of OSM (100ng/mL) for 24h. RNA was isolated, and qPCR was performed for the indicated genes. Student's t test (two tailed, unpaired) was performed in (B and H)**.** Data represent means ± SEM. $^{\#}P\leq 0.0001$, $^{\$}P\leq 0.0001$, ****$P\leq 0.0001$, ***$P\leq 0.001$, **$P\leq 0.01$, *$P\leq 0.05$.

Figure-S15, related to Figure 4 and 5

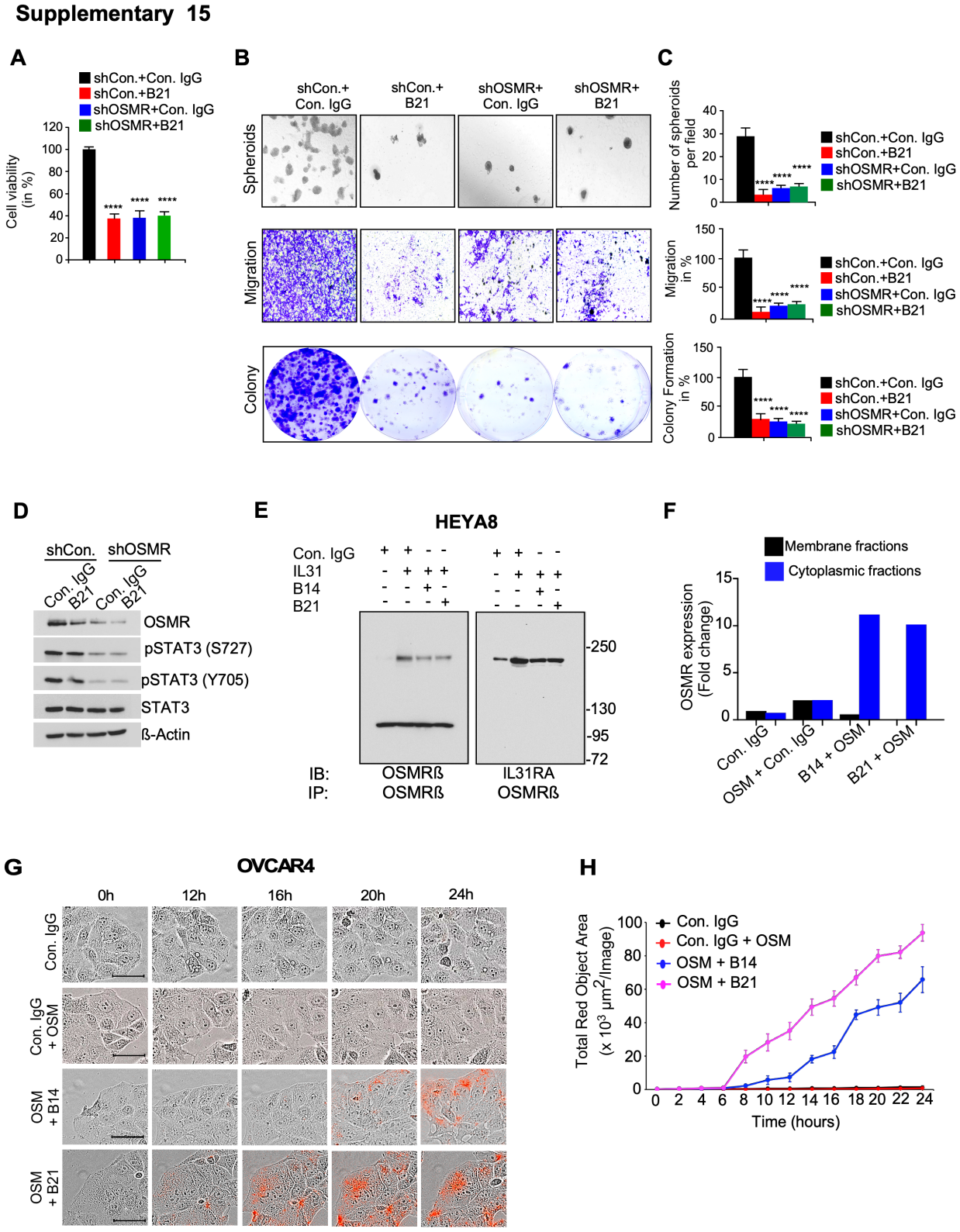

Fig. S15. Anti-OSMR antibodies were not able to induce any anti-proliferative or anti-migratory effects in OSMR-depleted cancer cells. A-D, HEYA8 cells stably knocked down of OSMR using shOSMR#1-lentiviral vector or control vectors were stimulated with B21 and control IgG antibodies (10 mg/mL each) for 48h. **A,** Cell viability was determined using CCK8 cell viability assay reagent after 48h. **B,** Representative images of 3D spheroid formation assay of stable HEYA8 cells prepared in (A) were cultured in ClonaCell media on low adherent plate in the presence of control IgG or B21 antibodies for 10 days (upper panel); scale bar, 500 mm. Representative images of transwell migration of HEYA8 cells in (A) were treated with control IgG and B21 antibodies for 12 h. Scale bar, 100 mm. Crystal violet staining was used to visualize the migrated cells (upper panel). Both control or OSMR-depleted HEYA8 cells (1200) were grown on 6-well culture plate with control IgG and B21 antibodies for 14 days. Colonies formed were stained using 0.5% crystal violet and imaged. **C,** (upper panel) Histogram represents the size of spheroids from 4 different fields per group on Day 10 of spheroid culture (lower panel). (middle panel) Histograms represents percentage of migrated cells from 3 different fields per group (lower panel). (lower panel) Histogram represents number of colonies formed in percentage with respect to shcontrol-HEYA8 cells treated with control IgG. **D,** Cell lysates were prepared from HEYA8 cells stably transfected with shControl and shOSMR and treated with control IgG and B21 antibodies and then western blot was performed for the indicated proteins. **E,** Dimerization assay performed in HEYA8 cells pre-treated with B14 or B21 mAbs for 4h, then stimulated with IL31 (100ng/mL) for 1h. Cell lysates were prepared after crosslinking with BS3 reagent and immunoprecipitated (IP) using anti-IL31RA or anti-OSMR antibody, then resolved on SDS/PAGE. Dimers and monomers (arrows) were detected using anti-OSMR and anti-IL31RA antibodies by immunoblot (IB). **F,** Histograms represent the protein levels of the indicated proteins in membrane and cytoplasmic fractions that were normalized to protein levels of Na, K-ATPase and LAMP1 from membrane and cytosolic fractions respectively as in Fig. 5D. **G,** Control IgG or B14 or B21 mAbs were labeled with Incucyte® Human FabFluor-pH Red Antibody Labeling Reagent and then added to OVCAR4 cells along with OSM (100 ng/mL) and incubated for 24h. Red fluorogenic signals released due to the low-acidic pH when the FabFluor-labelled anti-OSMR antibody internalized to lysosomes were quantitated. Time lapse imaging were performed to detect the fluorescence. Scale bar, 50mm. **H,**

Quantitative assessment of internalized OSMR antibody complex based on the total red dot area per image as evaluated using Incucyte S3 software. Data represent means ± SEM. Student's t test (two tailed, unpaired) and Dunnett's multiple comparison tests were performed to determine P-Value. ****P<0.0001

Figure-S16, related to Figure 6.

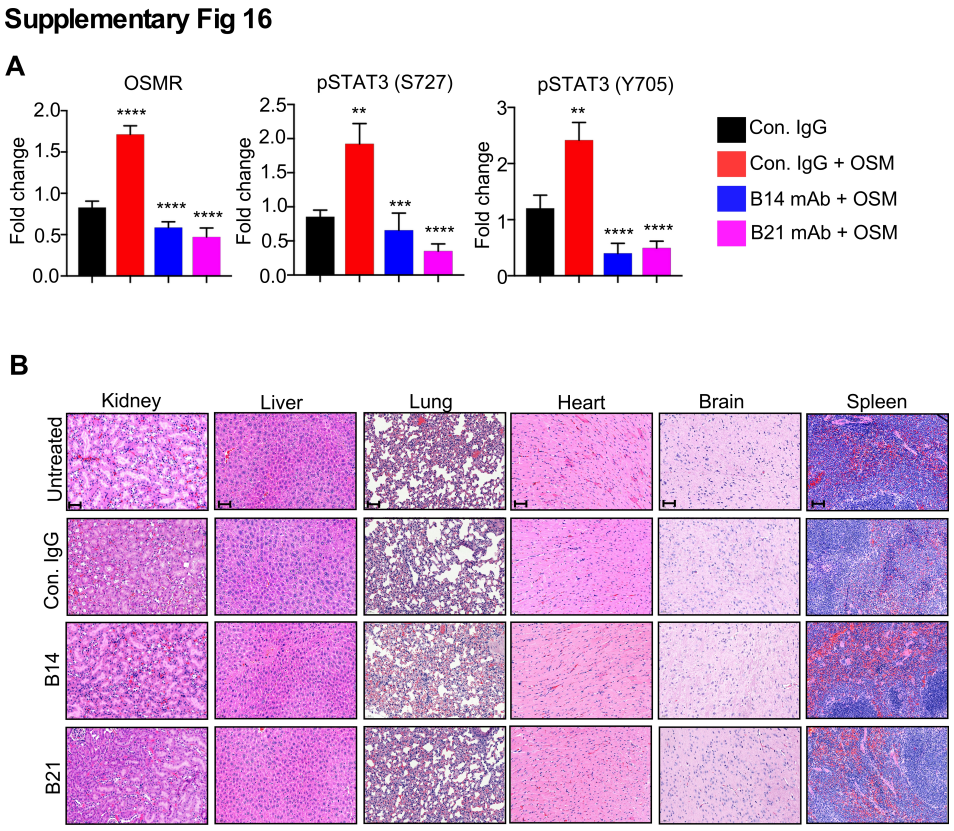

Fig. S16. Anti-OSMR antibodies reduced the incidence of tumor occurrence and metastasis of Ovarian cancer. A, Athymic nude mice were injected with HEYA8-Luc+ cells intraperitoneally. Mice were treated with OSM (250 ng/kg body weight) 30 min after the injections of control IgG, B14, B21, antibodies (10mg/kg body weight) intraperitoneally for 5 weeks (N=7/ group). Western blots were performed in triplicate using tissues from three representative mice from each group as in Fig. 6I and densitometric analysis was performed to determine the levels of indicated protein normalized to β-Actin in each group. **B,** Athymic nude mice (n=4) were injected with Control IgG, B14 and B21 mAbs (10mg/kg body weight each) for 5 weeks. Mice were sacrificed on 7th week and organs were collected, then H&E staining was performed from the sections of indicated organs

collected. Scale 50 μm. Data represent means ± SEM. Student's t test and Dunnett's multiple comparison test were performed. ****P≤ 0.0001, ***P≤0.001, **P≤0.01, *P≤0.05

Legend to Supplementary Material-1

Heatmap shows all the known ligand-receptor interactions between different cell types identified by CellPhoneDB in the OvD5-SS2 dataset.

Supplementary Table S1: Patient characteristics of the TMA cohort.

TMA data set Characteristics	Summary
Ovarian carcinoma patients	*N*=110
Age	48.27 ± 1.31 years
Gender	Female
Number of tumor histopathology image series	*N*=110
Number of histopathology image cores	*N*=150
Number of NAT cores	*N*=20
Number of Normal Ovarian tissue cores	*N*=10
Number of Metastatic tissue cores	N=10 (8%)
Number of Borderline tissue cores	N=7 (5.6%)
Number of Benign tissue cores	N=18 (14.4%)
Grade	
Grade 1	N=6 (5.45%)
Grade 2	N=23 (21%)
Grade 1-2	N=3 (2.72%)
Grade 3	N=20 (18.18%)
TMA data set Characteristics	**Summary**
Grade 4	N=0
Grade unavailable	N=58 (52.72%)
High Grade serous Ovarian carcinoma	N=23 (20.9%)
Low Grade serous Ovarian carcinoma	N=4 (3.64%)
Stage	
Stage I	N=29 (26.36%)
Stage II	N=26 (23.64%)
Stage III	N=24 (21.82%)

Supplementary Table S2: List of qPCR primers

Genes	Species	Direction	Sequence (5'→3')
OSMR	Human	Forward	CGC AGC AAG ACG GGA AAT TG
OSMR	Human	Reverse	GGG CGG GAG TTA CTG GAA AA
Osm	Mouse	Forward	CAG AAT CAG GCG AAC CTC ACG
Osm	Mouse	Reverse	AGC TCT CAG GTC AGG TGT GTT
IL31RA	Human	Forward	ACG TAC AAC CTC ACG GGG CT
IL31RA	Human	Reverse	TGG CCT TCT TCC ATC CGC CT
IL6ST	Human	Forward	TGT GAG TGG GAT GGT GGA AGG G
IL6ST	Human	Reverse	AGT GCA TGA GGT GGG GGT GT
STAT3	Human	Forward	GGA GGA GTT GCA GCA AAA AG
STAT3	Human	Reverse	TGT GTT TGT GCC CAG AAT GT
IL6RA	Human	Forward	CCA TGC AGG CAC TTA CTA CT
IL6RA	Human	Reverse	GGC AGT GGT ACT GAA GAA GAA
IL11RA	Human	Forward	CCG GAT TAA TGT GAC TGA GGT G
IL11RA	Human	Reverse	GGG TAA CCT GGT ACT GAC TCT A
LIFR	Human	Forward	CAT CAT CAG CGT AGT GGC TAA A
LIFR	Human	Reverse	GTA ATG CCA GGT GAG GAG AAT C
CNTFR	Human	Forward	CAG CAC ACA CCA TCA CAG A
CNTFR	Human	Reverse	GTC ACT CCA TGT CCC AAT CTC
IL27RA	Human	Forward	CTG TGG GTG ACA GCA TCT AC
IL27RA	Human	Reverse	CTT TCC ACC TCA GGG TGT TAT C
ACTB	Human	Forward	GTC ATT CCA AAT ATG AGA TGC GT
ACTB	Human	Reverse	GCT ATC ACC TCC CCT GTG TG
Actb	Mouse	Forward	GGC TGT ATT CCC CTC CAT CG
Actb	Mouse	Reverse	CCA GTT GGT AAC AAT GCC ATG T

Supplementary Table S3: Sequences of siRNAs used for transfections

Gene	Sequence
OSMR	siRNA#1: 5'-GUA ACU GCA UUC AAC UUG A-3'
OSMR	siRNA#2: 5'-CCA GAU CAG UAG GAU UGA A-3'
IL6ST	5'-CCU CAU GCA CUG UUG AUU A-3'
LIFR	5'-CCA CCU UCC AAA AUA GCG A-3'
IL31RA	5'-CAA UGA ACA CUA CUA ACC A-3'
IL6R	5'-CCA GUA GUG UCG GGA GCA A-3'
CNTFR	5'-GCC ACA AUG CCA CAG CUA U-3'
IL27RA	5'-GAG UUG GAC CCU UGG GCG A-3'
IL11RA	5'-CUG AGU UCU GGA GCC AGU A-3'

Supplementary Table S4: Catalogue Numbers of Plasmids

Plasmids	Catalogue No.	Sequence	Species	Company
MISSION® pLKO.1-shOSMR #1	TRCN0000058687, Clone ID: NM_003999.1-2459s1c1	5'-CCG GGC ATT GAT TGT GGA CAA CCT ACT CGA GTA GGT TGT CCA CAA TCA ATG CTT TTT G-3'	Human	Sigma Aldrich
MISSION® pLKO.1-puro-shOSMR #2	TRCN0000289933 Clone ID: NM_003999.1-2857s21c1	5'-CCG GCG AGT TGA CTA AGC CTA ACT ACT CGA GTA GTT AGG CTT AGT CAA CTC GTT TTT G-3'	Human	Sigma Aldrich
MISSION® pLKO.1-puro-shOsmr	TRCN0000339541 Clone ID: NM_011019	5'- TTG GAA CTG GAC GTC TGA TAT-3'	Mouse	Sigma Aldrich
MISSION® pLKO.1-puro Empty Vector control	SHC001V		Human	Sigma Aldrich
pUNO1-OSMR	#puno1-hosmr		Human	InvivoGen
pUNO1-Control	#puno1-mcs		Human	InvivoGen

Supplementary Table S5: Acute toxicity (athymic nude mice) Clinical biochemistry

	Liver function			Kidney function			Others
Parameters	**AST**	**ALT**	**ALP**	**TBIL**	**Albumin**	**TP**	**BW**
Group	U/L	U/L	U/L	mg/dL	g/dL	g/dL	gm
Normal Range[1,2]	*52-560*	*26-120*	*50-96*	*0.0-0.9*	*2.5-4.0*	*4.3-6.4*	*20-28*
Untreated	44.28 ± 3.25	19.86 ± 1.97	91.143 ± 9.54	0.14 ± 0.02	2.63 ± 0.23	4.26 ± 0.40	23.21 ± 0.40
Control IgG	327.43 ± 58.46	32.57 ± 3.05	94 ± 9.58	0.23 ± 0.02	2.77 ± 0.16	4.5 ± 0.3	23.26 ± 0.28
B14 mAb	294.14 ± 57.65	37 ± 3.84	87.28 ± 9.61	0.2 ± 0.0	2.8 ± 0.16	4.51 ± 0.25	22.65 ± 0.67
B21 mAb	305 ± 70.81	31.14 ± 3.38	85 ± 12.63	0.21 ± 0.01	2.63 ± 0.16	4.21 ± 0.28	23.09 ± 0.28

Aspartate Aminotransferase (AST); Alanine Aminotransferase (ALT); Alkaline Phosphatase (ALP); Total Bilirubin (TBIL); Total Protein (TP)**;** Body weight (BW)

Supplementary Table S6. Catalogue numbers and available Research Resource Identifier (RRID) number of reagents and software

KEY RESOURCES TABLE

REAGENT or RESOURCE	SOURCE	IDENTIFIER
Antibodies		
Anti-OSMRβ	Proteintech	Cat# 10982-1-AP; RRID: AB_2156583
Anti-OSMR	Sino Biologicals	Cat: 11226-RP02
Anti-LIFR	R&D Systems	Cat #AF-249-NA; RRID: AB_354420
anti-IL31RA	Thermo Fisher Scientific	Cat# PA5-47391; RRID: AB_2606511
anti-IL6ST (anti-gp130)	Santa Cruz Biotechnology	Cat# sc-376280; RRID: AB_10986409
pSTAT3 (S727) antibody	Cell Signaling Technology	Cat# 9134; RRID: AB_331589)
pSTAT3 (Y705) antibody	Cell Signaling Technology	Cat# 9145; RRID: AB_2491009
STAT3 antibody	Cell Signaling Technology	Cat# 9139; RRID: AB_331757
pJAK1 (Y1034/1035) antibody	Cell Signaling Technology	Cat# 74129; RRID: AB_2799851
JAK1 antibody	Cell Signaling Technology	Cat# 3344; RRID: AB_2265054
pJAK2 (Y1008) antibody	Cell Signaling Technology	Cat# 8082. RRID: AB_10949104
JAK2 antibody	Cell Signaling Technology	Cat# 74987. RRID: AB_2799862

Anti-β-Actin	Santa Cruz Biotechnology	Cat #sc 8432. RRID: AB_626630
Ki-67 antibody	Cell Signaling Technology	Cat #9027, RRID: AB_2636984
Anti-PCNA	Santa Cruz Biotechnology	Cat #sc-25280. RRID: AB_628109
BCL_{xL} antibody	Cell Signaling Technology,	Cat #2764. RRID: AB_2228008
BCL2 antibody	Cell Signaling Technology	Cat #15071. RRID: AB_2744528
Cytochrome c antibody	Cell Signaling Technology	Cat #11940. RRID: AB_2637071
p27 Kip1 antibody	Cell Signaling Technology	Cat #3686. RRID: AB_2077850
LAMP1 antibody	Cell Signaling Technology	Cat #15665. RRID: AB_2798750
Na,K-ATPase antibody	Cell Signaling Technology	Cat # #3010. RRID: AB_2060983
Anti-alpha 3 Sodium Potassium ATPase/ATP1A3 Antibody	Santa Cruz Biotechnology	Cat #sc-376967
Phospho-Akt (Ser473) antibody	Cell Signaling Technology	Cat #4058; RRID: AB_331168
Phospho-p44/42 MAPK (Erk1/2) (Thr202/Tyr204) antibody	Cell Signaling Technology	Cat #4376; RRID: AB_331772
p44/42 MAPK (Erk1/2) Antibody	Cell Signaling Technology	Cat #9102; RRID: AB_330744
Phospho-PI3 Kinase p85 (Tyr458)/p55 (Tyr199) antibody	Cell Signaling Technology	Cat# 4228, RRID: AB_659940

PI3 Kinase p85 antibody	Cell Signaling Technology	Cat #4257; RRID: AB_659889
Akt (pan) antibody	Cell Signaling Technology	Cat #2920. RRID: AB_1147620
Cleaved caspase3	Cell Signaling Technology	Cat #9661, RRID: AB_2341188
Anti-rabbit IgG, HRP-linked Antibody	Cell Signaling Technology	Cat # 7074, RRID: AB_2099233
Anti-mouse IgG, HRP-linked Antibody	Cell Signaling Technology	Cat # 7076, RRID: AB_330924
Brilliant Violet 510™ anti-mouse CD45 Antibody	BioLegend	Cat #103137. RRID: AB_2561392
APC anti-mouse CD140a Antibody	BioLegend	Cat #135908. RRID: AB_2043970
Alexa Fluor® 488 anti-mouse F4/80 Antibody	BioLegend	Cat #123120. RRID: AB_893479
CD326 (EpCAM) Monoclonal Antibody (G8.8), PE,	eBioscience	Cat #12-5791-82. RRID: AB_953615
IRDye® 680RD Donkey anti-Rabbit IgG Secondary Antibody	Li-Cor	Cat # 926-68073. RRID: AB_10954442
IRDye® 800CW Goat anti-Mouse IgG Secondary Antibody	Li-Cor	Cat #926-32210. RRID: AB_621842
Chemicals, Peptides, and Recombinant Proteins		
DMEM	Sigma Aldrich	Cat # D0819
MCDB 105	Sigma Aldrich	Cat # M6395
Medium 199	Sigma Aldrich	Cat # M4530
RPMI-1640	Sigma Aldrich	Cat #R8758

MEGM™ Mammary Epithelial Cell Growth Medium	Lonza	Cat #CC-3150
Eagle's Minimum Essential Medium with Earle's salts and non-essential amino acids	Sigma Aldrich	Cat #56416C
ClonaCell™-TCS Medium	Stem Cell Technologies	Cat #03814
HBSS	Thermo Fisher Scientific	Cat# 14060040
Recombinant EGF	Peprotech	AF-100-15
FBS (heat inactivated)	Atlanta Biologicals	Cat# H17112
FBS (non-heat inactivated)	ATCC	Cat # 30-2020
Antibiotic (Penicillin/Streptomycin)	Thermo Fisher Scientific	Cat #15140122
DMSO	Sigma Aldrich	Cat #D8418
Hydrocortisone	Sigma Aldrich	Cat #H0135
Bovine insulin	Sigma Aldrich	Cat #I0516
2-mercaptoethanol	Sigma Aldrich	Cat #M3148
Bovine pituitary extract	Life Technologies	Cat #13028014
Lipofectamine 2000	Invitrogen-Thermo Fisher Scientific	Cat #11668027
RNAiMax Transfection Reagent	Thermo Fisher Scientific	Cat #13778030
Cell Counting Kit-8 (CCK-8)	Dojindo, Japan	Cat #CK04-05
IncuCyte® Annexin V Red Reagent	Sartorius (Essen Bioscience)	Cat #4641
FabFluor (Red) reagent	Essen Bioscience	Cat #4722
Glutaraldehyde	Sigma Aldrich	Cat #G7651
Crystal Violet	Sigma Aldrich	Cat #C6158
Acetic acid	Sigma Aldrich	Cat #A6283

Trypsin	Thermo Fisher Scientific	Cat# 15400054
PBS	Sigma Aldrich	Cat# P5493
RIPA buffer	Santa Cruz Biotechnology	Cat# sc-24948A
Protein A/G Magnetic Beads	Thermo Fisher Scientific	Cat# 88802
Paraformaldehyde	Sigma Aldrich	Cat# 158127
Triton X 100	Sigma Aldrich	Cat# T8787
Glycine	Sigma Aldrich	Cat# G8898
Protease inhibitor cocktail	Sigma Aldrich	Cat# P8340
Dynabeads™ Protein A	Invitrogen	Cat# 10001D
10% Formalin fixative	VWR	Cat# 16004-121
Tween 20	Bio-Rad	Cat# 1706531
BSA	Sigma Aldrich	Cat# A7906
Ampicillin	Sigma Aldrich	Cat# A5354
LB Agar	Sigma Aldrich	Cat# L2897
LB Broth (Lennox)	Sigma Aldrich	Cat# L3022
Hematoxylin Solution, Harris Modified	Sigma Aldrich	Cat# HHS32-1L
IHC Antigen Retrieval solution	IHC World	Cat# IW-1100
Recombinant Human OSM Protein	Sino Biological	Cat# 10452-HNAH
Recombinant Human IL31 Protein	R & D Systems	Cat# 2824-IL
Recombinant Human LIF Protein	R & D Systems	Cat# 7734-LF
Recombinant Human OSMR	Sino Biologicals,	Cat# 11226-H08H
Trypan Blue	Sigma Aldrich	Cat# T8154
D-luciferin	Goldbio	Cat# LUCK-1G

Polybrene Transfection Reagent	Millipore	Cat# TR-1003
Puromycin	Thermo Fisher Scientific	Cat # A1113803
Blasticidin	InvivoGen	Cat #ant-bl-05
Mitomycin C	Sigma Aldrich	Cat #M4287
BS3	Thermo Fisher Scientific	Cat #21580
Critical Commercial Assay Kits		
MycoSensor PCR Assay kit	Agilent	Cat# 302109
Pierce BCA Protein Assay kit	Thermo Fisher Scientific	Cat# 23227
Mem-PER™ Plus Membrane Protein Extraction Kit	Thermo Fisher Scientific	Cat # 89842
RNeasy kit	Qiagen	Cat# 74104
iScriptTM Reverse Transcription Supermix for RT-qPCR	Bio-Rad	Cat# 1708841
iTaq Universal SYBR Green PCR Kit	Bio-Rad	Cat# 1725121
FITC Annexin V/Dead Cell Apoptosis Kit	BD Pharmingen	Cat# 556547
Proteome Profiler Human Apoptosis Array Kit	R&D Systems	Cat# ARY009
Human Phospho-Kinase Antibody Array kit	R&D Systems	Ca # ARY003B
Human OSM DuoSet ELISA	R & D Systems	Cat# DY295
Mouse OSM DuoSet ELISA	R & D Systems	Cat# DY495-05

Formalin-Fixed Paraffin-Embedded (FFPE) tissue array cores	US Biomax Inc.	Cat #OV1005bt and OV1004
Vectastain ABC-AP Kit	Vector Labs	Cat #AK-5000
Vector Red Alkaline Phosphatase Substrate Kit I	Vector Labs	Cat # SK-5100
Experimental Models: Cell Lines		
FTE187	MD Anderson Cancer Center	N/A
FTE188	MD Anderson Cancer Center	N/A
NIH-OVCAR3	ATCC/PBCF	Cat #300307/p690_NIH: Ovcar-3, RRID: CVCL_0465
OVCAR4	National Cancer Institute (NCI)	Cat# OVCAR-4, RRID: CVCL_1627
OVCAR5	National Cancer Institute (NCI)	Cat# OVCAR-5, RRID: CVCL_1628
OVCAR8	National Cancer Institute (NCI)	Cat# OVCAR-8, RRID: CVCL_1629
CaOV3	ATCC/PBCF	
SKOV3	ATCC/PBCF	Cat# HTB-77, RRID: CVCL_0532
HEYA8	MD Anderson Cancer Center, Texas, USA	N/A
MCAS	MD Anderson Cancer Center, Texas, USA	N/A
THP1	ATCC	Cat# TIB-202, RRID: CVCL_0006

HEK293-FT	Thermo Fisher Scientific	Cat# R70007
BR-Luc	University of California, Los Angeles, CA	N/A
GM15859	Coriell Institute for Medical Research, NJ, USA.	Cat# GM15859, RRID: CVCL_F624
RF24	VU University Medical Center, Amsterdam, Netherlands.	N/A
Biological Samples		
Human ovarian cancer tissues	Medical College of Wisconsin	Protocol Number: PRO00033433
Human ovarian surface epithelial (OSE) tissues	Medical College of Wisconsin	Protocol Number: PRO00033433
Human fallopian surface epithelial (FTE) tissues	Medical College of Wisconsin	Protocol Number: PRO00033433
Experimental Models: Organisms/Strains		
FVB/NJ - Homozygous mice	Charles River Laboratories	Cat #207
Athymic nude mice: CrTac: NCr-Foxn1nu	Envigo	Cat # Hsd: Athymic Nude-Foxn1nu
Oligonucleotides		
Primers for qPCR, see Table S4	Integrated DNA technologies	N/A

Software and Algorithms		
GraphPad Prism 7	GraphPad Software	https://www.graphpad.com/scientific- software/prism/
FlowJo Software	FlowJo	https://www.flowjo.com/
qPCR software	BioRad CFX Maestro	Cat# 12004110
Living Image Software (IVIS Imaging Systems) 4.7.3	Perkin Elmer	https://www.perkinelmer.com
Image J:	Image J	https://imagej.net/Coloc_2
Octet Software Version 10.0	ForteBio	https://www.fortebio.com
IncuCyte® S3 Software	Sartorius (Essen Bioscience)	https://www.essenbioscience.co

CONTACT FOR REAGENT AND RESOURCE INFORMATION: Further information and requests for resources and reagents should be directed to and will be fulfilled by the Lead Contact, Pradeep Chaluvally-Raghavan (pchaluvally@mcw.edu)

References:

1. Maranto C, Udhane V, Jia J, Verma R, Muller-Newen G, LaViolette PS*, et al.* Prospects for Clinical Development of Stat5 Inhibitor IST5-002: High Transcriptomic Specificity in Prostate Cancer and Low Toxicity In Vivo. Cancers (Basel) **2020**;12
2. Danneman P, Suckow MA, Brayton C, Suckow MA. The laboratory mouse. Boca Raton: Taylor & Francis; 2013. xvi, 234 p. p.